LIP, Lisbon, 29 November 2018

Modern Meson Spectroscopy: The Importance of Unitarity for Experiment, Lattice & Models

George Rupp

CeFEMA, Instituto Superior Técnico, Lisbon

Work with Eef van Beveren and Susana Coito

I. Introduction

II. Breit-Wigner mass, pole mass, and unitarity

III. Unitarised quark model for meson spectroscopy

IV. Lattice results for meson resonances

V. Threshold enhancements and controversial states

VI. Conclusions

Introduction

- Hadron spectroscopy aims at a better understanding of low-energy QCD, particularly the confinement and strong-decay mechanisms.
- Since most hadrons are resonances, many of which very broad, it is mandatory that experimental and theoretical approaches describe the same objects.
- According to principles from quantum field theory, resonance pole positions are unique, contrary to e.g. line shapes, which depend on the specific processes to produce resonances. This is the basis of the PDG tables.
- Nevertheless, experimental analyses of scattering and production data still employ Breit-Wigner (BW) or related parametrisations, which generally do not respect S-matrix unitarity and analyticity.
- Even modern lattice simulations now impose single- or even multichannel unitarity when describing meson resonances.
- Unitarised quark models and others that take dynamical effects of strong decay into account can lead to huge mass shifts when compared to predictions from static quark models (see next slide).

G. Rupp and E. van Beveren, Chin. Phys. C **41** (2017) 053104

Table 1. Negative real mass shifts from unquenching. Abbreviations: P,V,S=pseudoscalar, vector, scalar mesons, respectively; q=light quark. See text and Ref. [20] for further details.

Refs.	mesons	$-\Delta M$/MeV
[21]	charmonium	48–180
[22, 27]	light P, V	530–780, 320–500
[23, 28]	$\mathrm{q\bar{q}}$, $\mathrm{c\bar{q}}$, $\mathrm{c\bar{s}}$, $\mathrm{c\bar{c}}$, $\mathrm{b\bar{b}}$; P,V	$\approx$ 30–350
[29]	σ, κ, $\mathrm{f}_0(980)$, $\mathrm{a}_0(980)$	510–830
[29]	standard S (1.3–1.5 GeV)	~ 0
[30]	$\rho(770)$, $\phi(1020)$	328, 94
[24]	$\mathrm{D}^{\star}_{s0}(2317)$, $\mathrm{D}^{\star}_{0}(2400)$	260, 410
[31]	$\mathrm{D}^{\star}_{s0}(2317)$, $\mathrm{D}^{\star}_{s}(2632)$	173, 51
[32]	charmonium	165–228
[33]	charmonium	416–521
[34]	X(3872)	$\approx$100
[35]	$\mathrm{c\bar{q}}$, $\mathrm{c\bar{s}}$; $J^P=1^+$	4–13, 5–93

Resonances: Breit-Wigner (BW) approximation:

$$Ampl = \frac{C}{E - M_{BW} + i\Gamma_{BW}/2}$$

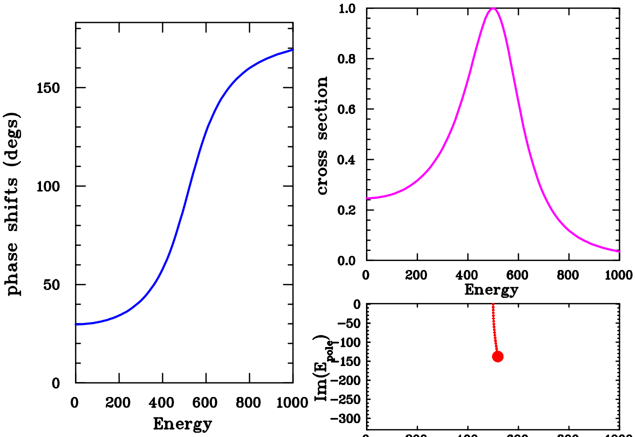

One channel scattering

- $S(k) = \frac{D(-k)}{D(k)} = e^{2i\delta}$, $|S(k)| = 1$
- $D(k) = (k - k_j)$
- $D(-k) = (-k - k_j)$
- But $|S(k)| \neq 1$ so

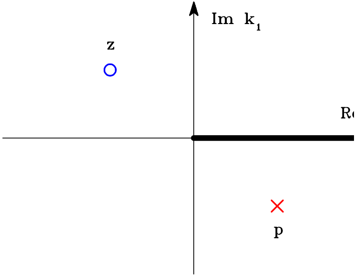

One channel scattering

- $S(k) = \frac{D(-k)}{D(k)} = e^{2i\delta}$, $|S(k)| = 1$
- $D(k) = (k - k_j)$
- $D(-k) = (-k - k_j)$
- But $|S(k)| \neq 1$ so
- $D(k) = (k - k_j)(k + k_j^*)$
- $D(-k) = (-k - k_j)(-k + k_j^*)$
- then $|S(k)| = 1$
- and $\delta = (-\alpha - \beta + \gamma + \omega)/2$

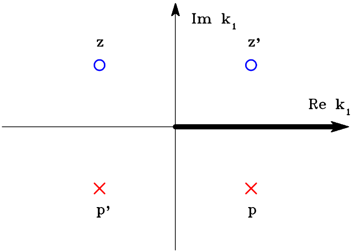

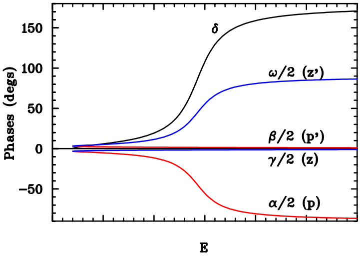

$$E = 2\sqrt{(\pm k)^2 + m^2}$$

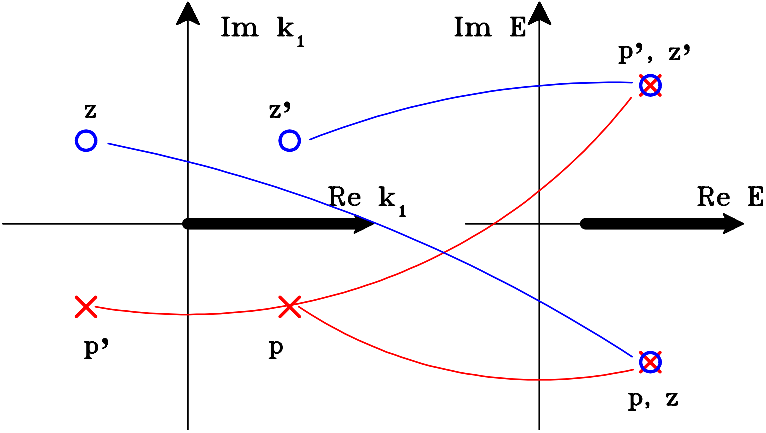

Pole and mass of a resonance

- Let's imagine good fit of an amplitude to the data —> mass M_{BW} at $\delta = 90^o$
  - Amplitude A_{BW} has a single pole at $k = a - ib$ then $\delta = ArcTan(\frac{b}{k-a})$ and $M_{BW} = 2\sqrt{a^2 + m^2}$ but then $|S| \neq 1$
  - Amplitude A_R has two symmetric poles at $k = c - id$ and $k = -c - id$ then $|S| = 1$, $\delta = ArcTan(\frac{2dk}{k^2 - c^2 - d^2})$ and $M_{BW} \neq 2\sqrt{c^2 + m^2}$

$\rho(770)$ pole mass vs. Breit-Wigner mass obeying unitarity

$$k_{\text{pole}} = c - id \quad (\text{and} \ -c - id) \tag{1}$$

$$M_{\text{BW}} : \tan\delta = \frac{2dk}{c^2 + d^2 - k^2} = \infty \ \Rightarrow \ k_{\text{BW}} = \sqrt{c^2 + d^2} \tag{2}$$

$$M_{\text{BW}}^2 = 2\sqrt{c^2 + d^2 + m^2} \tag{3}$$

$$E_{\text{pole}} = 2\sqrt{k_{\text{BW}}^2 + m^2} = 2\sqrt{c^2 - d^2 + m^2 - 2icd} \tag{4}$$

$$M_{\text{BW}}^2 + \text{Re}(E_{\text{pole}}^2) = 8(c^2 + m^2) \tag{5}$$

$$M_{\text{BW}}^2 - \text{Re}(E_{\text{pole}}^2) = 8d^2 \tag{6}$$

$$\text{Im}(E_{\text{pole}}^2) = -8cd \tag{7}$$

$$E_{\text{pole}} = M_{\text{pole}} - i\Gamma/2 \ \Rightarrow \ E_{\text{pole}}^2 = M_{\text{pole}}^2 - \Gamma^2/4 - i\Gamma M_{\text{pole}} \tag{8}$$

$$\text{Im}(E_{\text{pole}}^2) = -\Gamma M_{\text{pole}} = -8cd \tag{9}$$

From Eqs. (5), (6), (9) we get after some trivial algebra

$$M_{\text{pole}} = \sqrt{\sqrt{(M_{\text{BW}}^2 - 4m^2)^2 - 4m^2\Gamma^2} + 4m^2 - \frac{\Gamma^2}{4}} \tag{10}$$

Example: $\rho^0(770) \to \pi^+\pi^-$

PDG:

$M_{\rho^0} = 775.26$ MeV, $\Gamma_{\rho^0} = 147.8$ MeV, $m_{\pi^\pm} = 139.57$ MeV

Substitution in Eq. (10) gives $M_{\text{pole}} = 770.67$ MeV

- So even for a completely unitary description of a moderately broad single-channel resonance, BW mass and pole mass differ by almost 5 MeV.
- When a simple, non-unitary BW parametrisation is used to fit the P-wave $\pi\pi$ phase shifts, this difference can become as large as 10 MeV (Robert Kaminski dixit), making the 5-digit accuracy of the $\rho(770)$ mass in the PDG tables very questionable.
- When one is dealing with a very broad and highly inelastic resonance, possibly overlapping with others, this discrepancy can even become larger than 100 MeV (see next slide).

E. Bartoš, S. Dubnička, A. Liptaj, A. Z. Dubničková, and R. Kamiński, Phys. Rev. D **96** (2017) 113004

TABLE II. The values of ρ meson parameters obtained from fits of BESIII + *BABAR* data [1,2] on the total cross section of the $e^+e^- \to \pi^+\pi^-$ process with Gounaris-Sakurai and Unitary& Analytic pion EM FF models to be compared to PDG values.

Parameter	PDG value (MeV)	Gounaris-Sakurai (MeV)	Unitary & Analytic (MeV)
m_ρ	775.26 ± 0.25	774.81 ± 0.01	763.88 ± 0.04
$m_{\rho'}$	1465.00 ± 25.00	1497.70 ± 1.07	1326.35 ± 3.46
$m_{\rho''}$	1720.00 ± 20.00	1848.40 ± 0.09	1770.54 ± 5.49
Γ_ρ	149.10 ± 0.80	149.22 ± 0.01	144.28 ± 0.01
$\Gamma_{\rho'}$	400.00 ± 60.00	442.15 ± 0.54	324.13 ± 12.01
$\Gamma_{\rho''}$	250.00 ± 100.00	322.48 ± 0.69	268.98 ± 11.40
χ^2/ndf		0.981 [14 parameters]	1.842 [11 parameters]

Resonance-Spectrum Expansion

(EvB & GR, Annals Phys. **324** (2009) 1620)

$\Rightarrow$ Building blocks of (non-exotic) RSE are:

$V =$

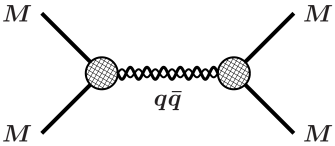

$V\Omega V =$

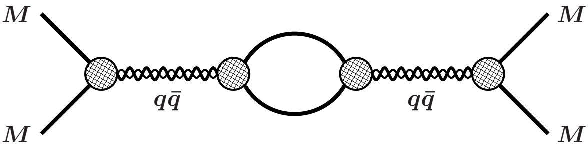

- V is the effective two-meson potential;
- Ω is the two-meson loop function;
- the blobs are the ${}^3P_0$ vertex functions, modelled by a spherical δ shell in r space, i.e., a spherical Bessel function in p space;
- the wiggly lines stand for s-channel exchanges of infinite towers of $q\bar{q}$ states, i.e., a kind of Regge propagators.

⇒ For N meson-meson channels and several $q\bar{q}$ channels:

$$\begin{aligned} V_{ij}^{(L_i,L_j)}(p_i,p_j';E) &= \lambda^2 r_0\, j_{L_i}^i(p_i r_0)\, j_{L_j}^j(p_j' r_0) \sum_{\alpha=1}^{N_{q\bar{q}}} \sum_{n=0}^{\infty} \frac{g_i^{(\alpha)}(n) g_j^{(\alpha)}(n)}{E - E_n^{(\alpha)}} \\ &\equiv \mathcal{R}_{ij}(E)\, j_{L_i}^i(p_i r_0)\, j_{L_j}^j(p_j' r_0)\ . \end{aligned}$$

⇒ The closed-form off-energy-shell T-matrix then reads

$$T_{ij}^{(L_i,L_j)}(p_i,p_j';E) =$$

$$-2\lambda^2 r_0 \sqrt{\mu_i p_i \mu_j' p_j'}\, j_{L_i}^i(p_i r_0) \sum_{m=1}^{N} \mathcal{R}_{im}(E)\ \left\{[\mathbb{1} - \Omega\,\mathcal{R}]^{-1}\right\}_{mj}\ j_{L_j}^j(p_j' r_0)\ ,$$

$$\Omega\ =\ -2i\lambda^2 r_0\, \mathrm{diag}\left(j_{L_n}^n(k_n r_0) h_{L_n}^{(1)n}(k_n r_0) \right)\ .$$

⇒ The corresponding unitary and symmetric S-matrix is given by

$$S_{ij}^{(L_i,L_j)}(k_i,k_j';E)\ =\ \delta_{ij}\ +\ 2iT_{ij}^{(L_i,L_j)}(k_i,k_j';E)\ .$$

Complex masses in the S-matrix

S. Coito, G. Rupp, E. van Beveren, Eur. Phys. J. C **71** (2011) 1762;
T. Takagi, Japan J. Math. **1** (1924) 82.

With complex masses, S ceases to be unitary. Nevertheless, S is always symmetric, so can be decomposed via Takagi factorisation:

$$S \;=\; VDV^T \;, \tag{11}$$

with V unitary and D a real non-negative diagonal matrix. Then

$$S^\dagger S = (V^T)^\dagger DV^\dagger VDV^T = (V^T)^\dagger D^2 V^T = U^\dagger D^2 U \;, \tag{12}$$

where $U \equiv V^T$ is also unitary. So $D = \sqrt{US^\dagger SU^\dagger}$. Moreover, since $S = \mathbb{1} + 2iT$ is manifestly non-singular, the eigenvalues of $S^\dagger S$ are even all nonzero and U is unique. Thus, we may define

$$S' \;\equiv\; SU^\dagger D^{-1} U \;. \tag{13}$$

Then, using Eq. (11) and $V = U^T$, we have

$$S' \;=\; U^T DUU^\dagger D^{-1} U \;=\; U^T U \;, \tag{14}$$

which is obviously symmetric and, as

$$(U^T U)^\dagger = U^\dagger (U^\dagger)^T = U^{-1}(U^{-1})^T = (U^T U)^{-1} \;, \tag{15}$$

also unitary. So S' can be defined as the S-matrix for a scattering process with complex masses in the asymptotic states.

E. van Beveren, T. A. Rijken, K. Metzger, C. Dullemond, G. Rupp, J. E. Ribeiro, Z. Phys. C **30** (1986) 615 [arXiv:0710.4067 [hep-ph]]

Abstract

A unitarized nonrelativistic meson model which is successful for the description of the heavy and light vector and pseudoscalar mesons yields, in its extension to the scalar mesons but for the same model parameters, a complete nonet below 1 GeV. In the unitarization scheme, real and virtual meson-meson decay channels are coupled to the quark-antiquark confinement channels. The flavor-dependent harmonic-oscillator confining potential itself has bound states $\epsilon(1.3\text{ GeV})$, $S(1.5\text{ GeV})$, $\delta(1.3\text{ GeV})$, $\kappa(1.4\text{ GeV})$, similar to the results of other bound-state $q\bar{q}$ models. However, the full coupled-channel equations show poles at $\epsilon(0.5\text{ GeV})$, $S(0.99\text{ GeV})$, $\delta(0.97\text{ GeV})$, $\kappa(0.73\text{ GeV})$. Not only can these pole positions be calculated in our model, but also cross sections and phase shifts in the meson-scattering channels, which are in reasonable agreement with the available data for $\pi\pi$, $\eta\pi$ and $K\pi$ in S-wave scattering.

- Unitarised quark-meson model, with all parameters fixed from previous work.
- All decay channels with pseudoscalar and vector mesons included.
- Poles of light scalar mesons found at: $f_0(470 - i208)$, $K_0^*(727 - i263)$, $a_0(968 - i28)$, $f_0(994 - i20)$.
- Additional poles found for $f_0(1370)$, $K_0^*(1430)$, $a_0(1450)$, $f_0(1500)$, at reasonable values.
- Moreover, S-wave scattering data were reasonably reproduced.

E. van Beveren, T. A. Rijken, K. Metzger, C. Dullemond, G. Rupp, and J. E. Ribeiro, Z. Phys. C **30** (1986) 615

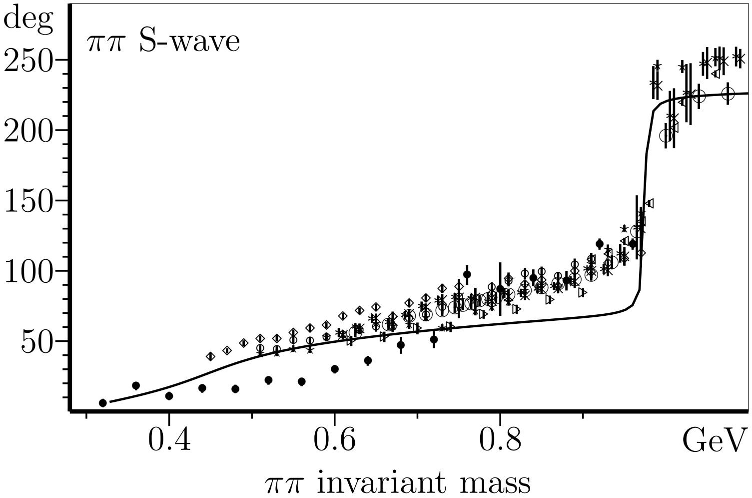

Poles predicted at **(470 − i208)** MeV and **(990 − i20)** MeV.

$D_{s0}^*(2317)$ & $D_0^*(2300\text{–}2400)$

E. van Beveren & G. Rupp, Phys. Rev. Lett. **91** (2003) 012003

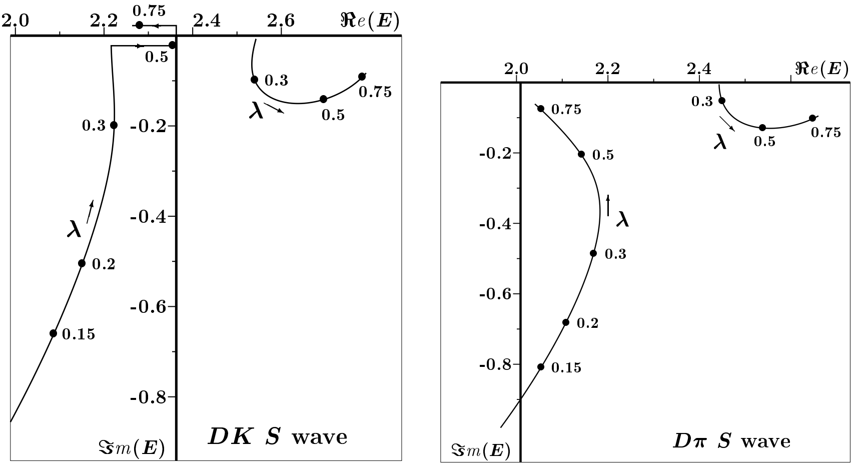

S. Coito, G. Rupp, and E. van Beveren, Phys. Rev. D **84** (2011) 094020

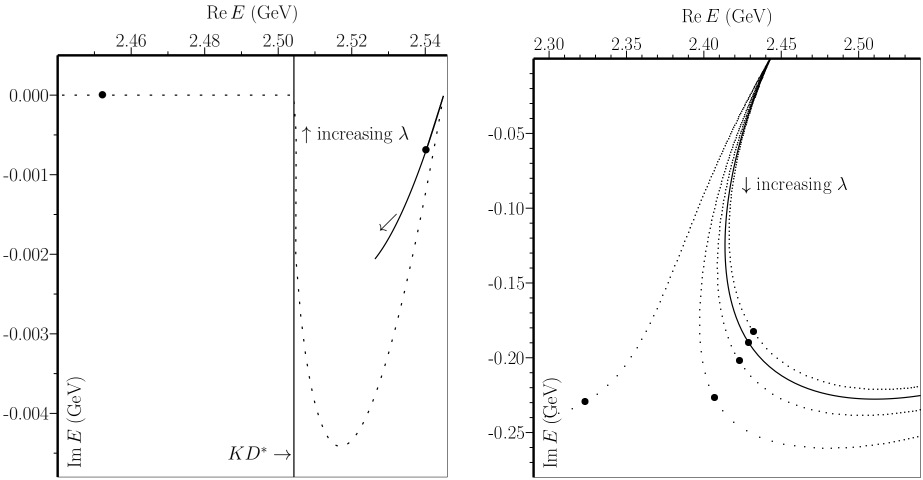

D_{s1}(2460) and **D_{s1}(2536)**

D_1(2430)

χ_{c1}(3872) as an intrinsic or a dynamical unitarised $2\,^3P_1$ $c\bar{c}$ state

S. Coito, G. Rupp, and E. van Beveren

Eur. Phys. J. C **73** (2013) 2351 [arXiv:1212.0648 [hep-ph]]

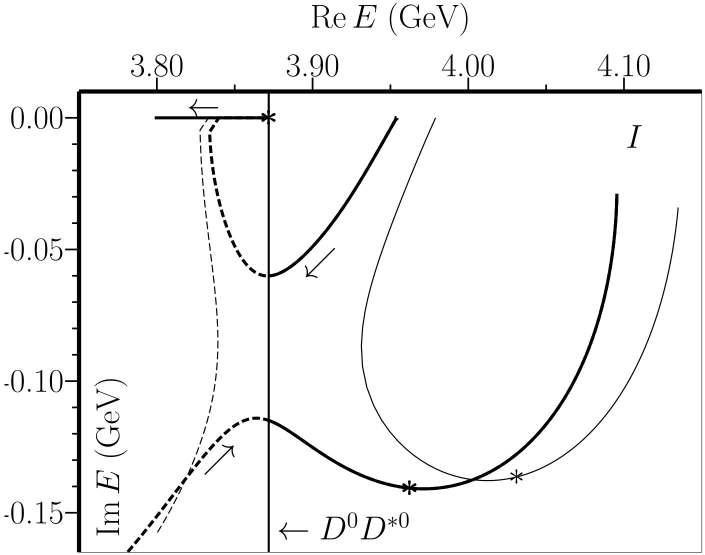

Wave function of $\chi_{c1}(3872)$ as a unitarised $2\,^3P_1$ $c\bar{c}$ state

M. Cardoso, G. Rupp, and E. van Beveren

Eur. Phys. J. C **75** (2015) 26 [arXiv:1411.1654 [hep-ph]]

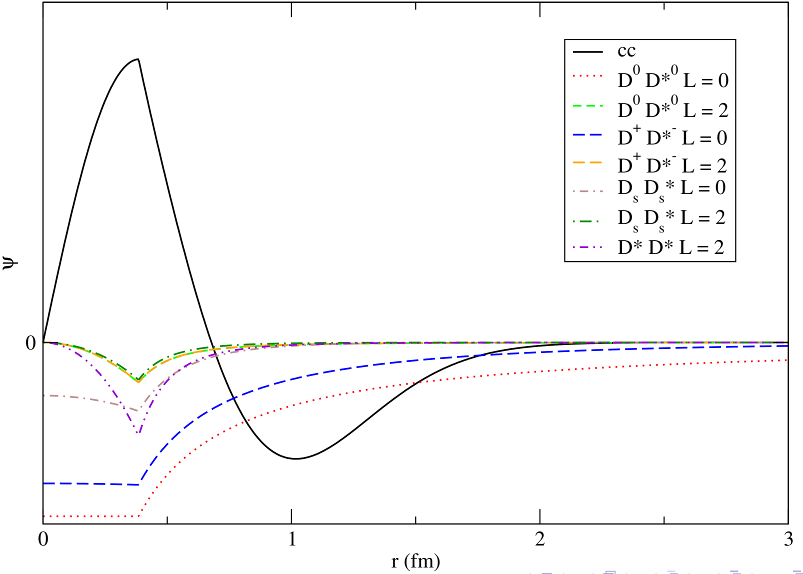

M. Padmanath, C. B.Lang, and S. Prelovsek Phys. Rev. D **92** (2015) 034501

We perform a lattice study of charmonium-like mesons with $J^{PC} = 1^{++}$ and three quark contents $\bar{c}c\bar{d}u$, $\bar{c}c(\bar{u}u + \bar{d}d)$ and $\bar{c}c\bar{s}s$, where the later two can mix with $\bar{c}c$. This simulation with $N_f = 2$ and $m_\pi \simeq 266$ MeV aims at the possible signatures of four-quark exotic states. We utilize a large basis of $\bar{c}c$, two-meson and diquark-antidiquark interpolating fields, with diquarks in both antitriplet and sextet color representations. A lattice candidate for $X(3872)$ with $I = 0$ is observed very close to the experimental state only if both $\bar{c}c$ and $D\bar{D}^*$ interpolators are included; the candidate is not found if diquark-antidiquark and $D\bar{D}^*$ are used in the absence of $\bar{c}c$. No candidate for neutral or charged $X(3872)$, or any other exotic candidates are found in the $I = 1$ channel. We also do not find signatures of exotic $\bar{c}c\bar{s}s$ candidates below 4.2 GeV, such as $Y(4140)$. Possible physics and methodology related reasons for that are discussed. Along the way, we present the diquark-antidiquark operators as linear combinations of the two-meson operators via the Fierz transformations.

... *"In the physical world with* $\mathbf{N_c = 3}$*, it is argued that tetraquarks could exist at subleading orders [46] of large* $\mathbf{N_c}$ *QCD. However, in the presence of the leading order two-meson terms, one should take caution in interpreting the nature of the levels purely based on their overlap factors onto various four-quark interpolators."* ...

TABLE III. Mass of $X(3872)$ with respect to $m_{\mathrm{s.a.}}$ and the $D_0\bar{D}_0^*$ threshold. Our estimates are from the correlated fits to the corresponding eigenvalues using single exponential fit form with and without diquark-antidiquark operators. Results from previous lattice QCD simulations [17,18] and experiment are also presented.

$X(3872)$	$m_X - m_{\mathrm{s.a.}}$	$m_X - m_{D_0} - m_{D_0^*}$
Lat.	816(15)	−8(15)
Lat.$-O^{4q}$	815(8)	−9(8)
LQCD [17]	815(7)	−11(7)
LQCD [18]	$\cdots$	−13(6)
Experiment	803(1)	−0.11(21)

... *"These results are in agreement with a possible interpretation of* **X(3872)**, *where its properties are due to the accidental alignment of a* $\mathbf{c\bar{c}}$ *state with the* $\mathbf{D^0\bar{D}^{\star 0}}$ *threshold [49,50], but we cannot rule out other options."* ...

G. Engel, C. Lang, D. Mohler, A. Schäfer, PoS Hadron2013 (2013) 118 [arXiv:1311.6579 [hep-ph]: **K$^{\star\prime}$** level above 1.6 GeV:

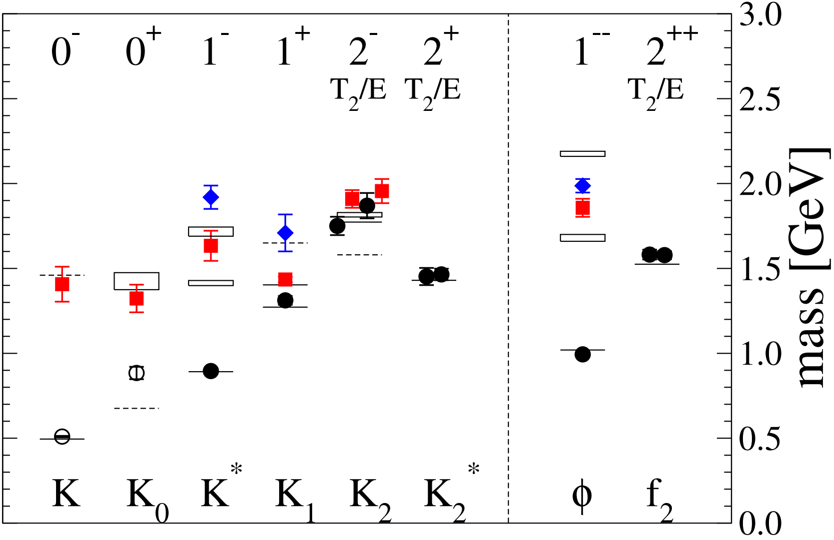

- However, $\mathbf{K^{\star\prime}}$ resonance at $\mathbf{(1.33 \pm 0.02)}$ GeV (Exp. 1.41):

S. Prelovsek, L. Leskovec, C. Lang, D. Mohler, Phys. Rev. D **88** (2013) 054508

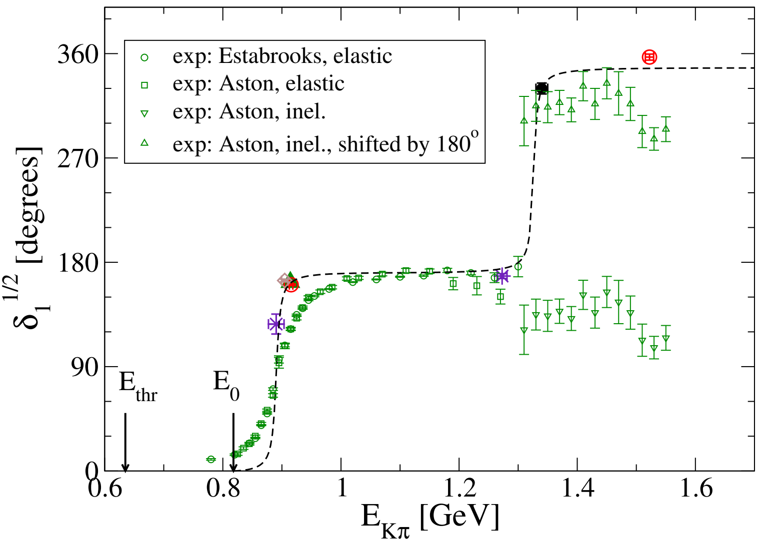

Production amplitudes in the RSE formalism

EvB & GR, Annals Phys. **323** (2008) 1215

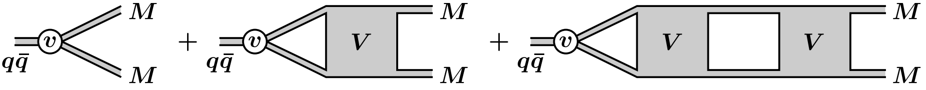

$$a(\alpha \to i) = \frac{\lambda}{\sqrt{\pi}} \sum_{\ell,m} (-i)^{\ell} j_{\ell}(p_i r_0) Y_m^{(\ell)}(\hat{p}_i) Q_{\ell_{q\bar{q}}}^{(\alpha)}(E)$$

$$\times \left\{ \frac{g_{\alpha i}}{\mathcal{D}^{(\ell)}} + i \sum_{v \neq i} \mu_v p_v h_{\ell}^{(1)}(p_v r_0) \left[g_{\alpha i} \frac{t_{\ell}(v \to v)}{j_{\ell}(p_v r_0)} - g_{\alpha v} \frac{t_{\ell}(i \to v)}{j_{\ell}(p_i r_0)} \right] \right\}$$

$$\mathcal{D}^{(\ell)}(E) = 1 + 2i\lambda^2 \sum_v g_v^2 \left\{ \sum_{n=0}^{\infty} \frac{\left| F_{c\bar{c}}^{(n)}(r_0) \right|^2}{E - E_n} \right\} \mu_v p_v j_{\ell}(p_v r_0) h_{\ell}^{(1)}(p_v r_0)$$

ψ(3770)

BES reported an *"anomalous line shape"* of the ψ(3770) resonance in arXiv:0807.0494 [hep-ex]:

> *"The anomalous line-shape may be explained by two possible enhancements of the inclusive hadron production near the center-of-mass energies of 3.764 GeV and 3.779 GeV, indicating that either there is likely a new structure in addition to the ψ(3770) resonance around 3.773 GeV, or there are some physics effects reflecting the* **DD** *production dynamics."*

Our explanation in EvB, GR, Phys. Rev. D **80** (2009) 074001:

- Opening of $\mathbf{D\bar{D}}$ threshold in $\mathbf{e^+e^-}$ produces a broad bump in the production cross section (Bessel function).
- On top of the structure there is a Breit-Wigner resonance, with $\mathbf{M = 3781}$ MeV and $\mathbf{\Gamma = 17}$ MeV, i.e., narrower and a little bit heavier than in the PDG tables.
- See figure on next slide.

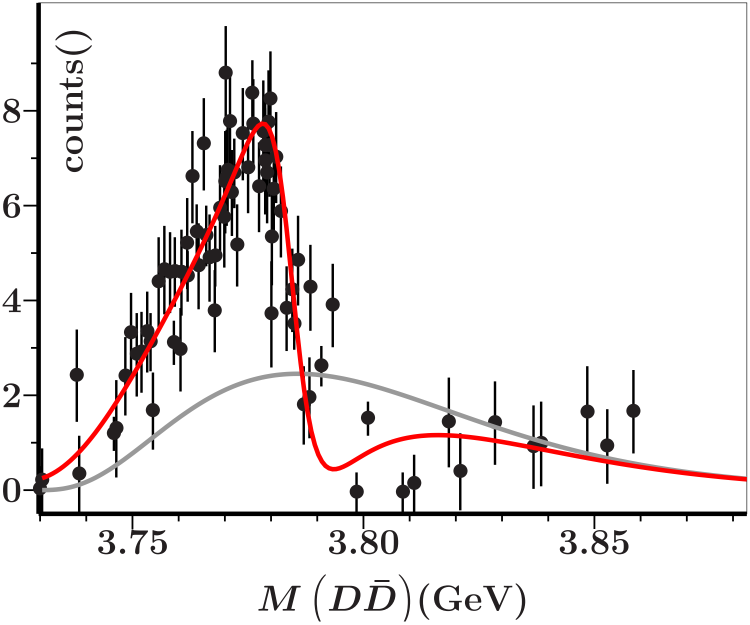

counts()
8
6
4
2
0
3.75
3.80
3.85
$M\left(D\bar{D}\right)$(GeV)

$\psi(4260)$ decay modes in the PDG-2018 Meson Listings

M. Tanabashi *al.* (Particle Data Group)
Phys. Rev. D **98** (2018) 030001

	Mode	Fraction (Γ_i/Γ)
Γ_1	e^+e^-	
Γ_2	$J/\psi\pi^+\pi^-$	seen
Γ_3	$J/\psi f_0(980)$, $f_0(980) \to \pi^+\pi^-$	seen
Γ_4	$Z_c(3900)^\pm\pi^\mp$, $Z_c^\pm \to J/\psi\pi^\pm$	seen
Γ_5	$J/\psi\pi^0\pi^0$	seen
Γ_6	$J/\psi K^+K^-$	seen
Γ_7	$J/\psi K_S^0 K_S^0$	not seen
Γ_8	$J/\psi\eta$	not seen
Γ_9	$J/\psi\pi^0$	not seen
Γ_{10}	$J/\psi\eta'$	not seen
Γ_{11}	$J/\psi\pi^+\pi^-\pi^0$	not seen
Γ_{12}	$J/\psi\eta\pi^0$	not seen
Γ_{13}	$J/\psi\eta\eta$	not seen
Γ_{14}	$\psi(2S)\pi^+\pi^-$	not seen
Γ_{15}	$\psi(2S)\eta$	not seen
Γ_{16}	$\chi_{c0}\omega$	not seen
Γ_{17}	$\chi_{c1}\pi^+\pi^-\pi^0$	not seen
Γ_{18}	$\chi_{c2}\pi^+\pi^-\pi^0$	not seen
Γ_{19}	$h_c(1P)\pi^+\pi^-$	not seen
Γ_{20}	$\phi\pi^+\pi^-$	not seen
Γ_{21}	$\phi f_0(980) \to \phi\pi^+\pi^-$	not seen
Γ_{22}	$D\overline{D}$	not seen
Γ_{23}	$D^0\overline{D}^0$	not seen
Γ_{24}	D^+D^-	not seen
Γ_{25}	$D^*\overline{D}$+c.c.	not seen
Γ_{26}	$D^*(2007)^0\overline{D}^0$ +c.c.	not seen
Γ_{27}	$D^*(2010)^+D^-$ +c.c.	not seen
Γ_{28}	$D^*\overline{D}^*$	not seen
Γ_{29}	$D^*(2007)^0\overline{D}^*(2007)^0$	not seen
Γ_{30}	$D^*(2010)^+D^*(2010)^-$	not seen
Γ_{31}	$D\overline{D}\pi$+c.c.	
Γ_{32}	$D^0D^-\pi^+$+c.c. (excl. $D^*(2007)^0\overline{D}^{*0}$ +c.c., $D^*(2010)^+D^-$ +c.c.)	not seen
Γ_{33}	$D\overline{D}^*\pi$+c.c. (excl. $D^*\overline{D}^*$)	not seen
Γ_{34}	$D^0D^{*-}\pi^+$+c.c. (excl. $D^*(2010)^+D^*(2010)^-$)	not seen
Γ_{35}	$D^0D^*(2010)^-\pi^+$+c.c.	not seen
Γ_{36}	$D^*\overline{D}^*\pi$	not seen
Γ_{37}	$D_s^+D_s^-$	not seen
Γ_{38}	$D_s^{*+}D_s^-$ +c.c.	not seen
Γ_{39}	$D_s^{*+}D_s^{*-}$	not seen
Γ_{40}	$p\overline{p}$	not seen
Γ_{41}	$p\overline{p}\pi^0$	not seen
Γ_{42}	$K_S^0K^\pm\pi^\mp$	not seen
Γ_{43}	$K^+K^-\pi^0$	not seen
	Radiative decays	
Γ_{44}	$\eta_c(1S)\gamma$	possibly
Γ_{45}	$\chi_{c1}\gamma$	not seen
Γ_{46}	$\chi_{c2}\gamma$	not seen
Γ_{47}	$\chi_{c1}(3872)\gamma$	seen

$\psi(4260)$ as a non-resonant **c$\bar{\text{c}}$** structure from inelasticities

E. van Beveren, G. Rupp, and J. Segovia

Phys. Rev. Lett. **105** (2010) 102001 [arXiv:1005.1010 [hep-ph]]

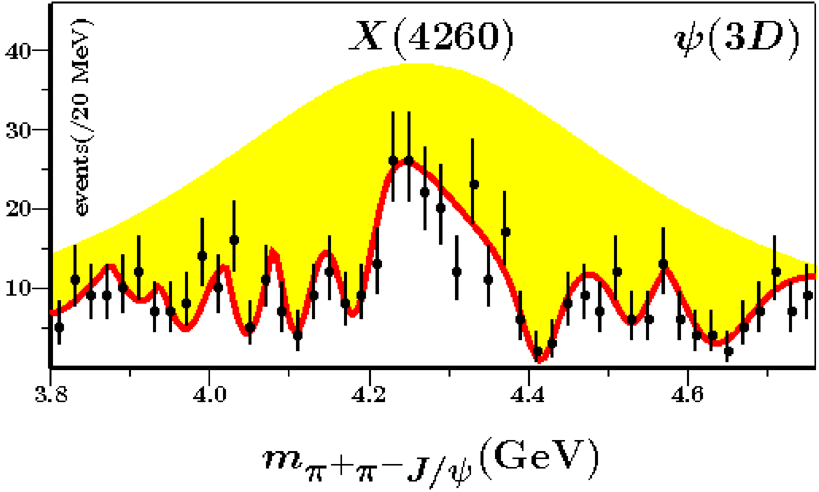

$\psi(4660)$ as a $\Lambda_c\bar{\Lambda}_c$ threshold enhancement in BABAR data

E. van Beveren, X. Liu, R. Coimbra, and G. Rupp

Europhys. Lett. **85** (2009) 61002 [arXiv:0809.1151 [hep-ph]]

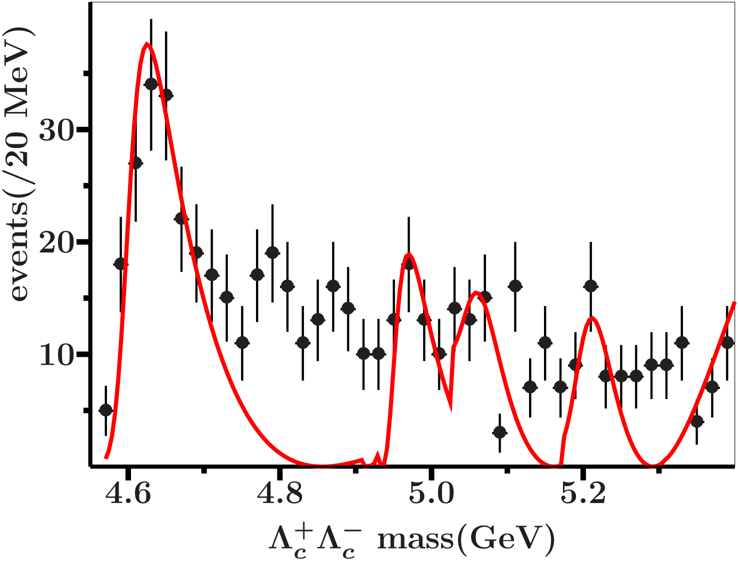

Alternative vector $\mathbf{b\bar{b}}$ spectrum from threshold enhancements

E. van Beveren and G. Rupp, arXiv:0910.0967 [hep-ph]

Also see: EvB & GR, Phys. Rev. D **80** (2009) 074001

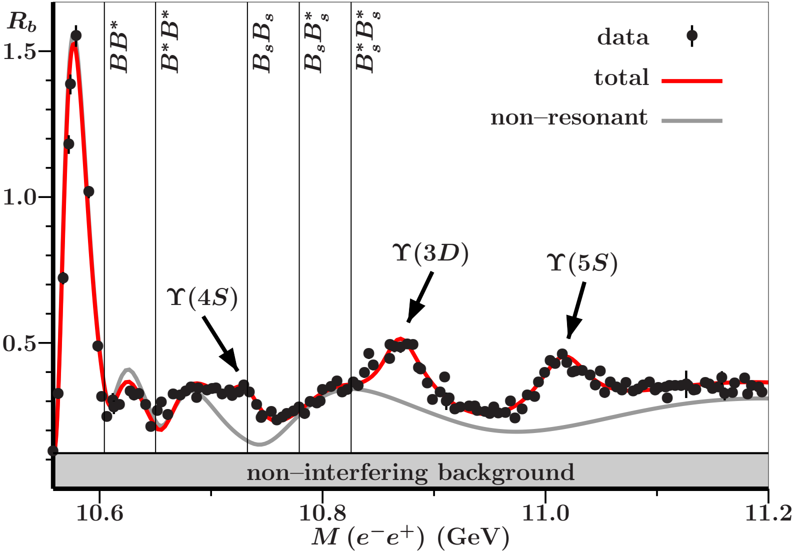

Conclusions

- Breit-Wigner parametrisations of meson resonances can give rise to large and difficult to control discrepancies when compared to unitary approaches.
- In unquenched lattice computations of meson resonances, the dynamical effects of decay in a unitary framework can lead to large corrections, too. Even for (quasi-)bound states such contributions may be sizeable.
- Also in quark models of mesons, unitarisation — or at least accounting for mass shifts due to strong decay — produce a strong distortion of the confinement-only spectrum.
- For real progress in meson spectroscopy, the three approaches — experiment, lattice, and models — should converge towards a unified description of meson resonances in terms of pole positions in a multichannel **S**-matrix.
- A highly underestimated and still somewhat underdeveloped issue in the description of hadronic peaks is the mechanism of threshold enhancements, which can mimic states commonly interpreted as genuine resonances.